

Brassinosteroids Regulate Grain Filling in Rice

Chuan-yin Wu,^a Anthony Trieu,^a Parthiban Radhakrishnan,^a Shing F. Kwok,^a Sam Harris,^a Ke Zhang,^a Jiulin Wang,^b Jianmin Wan,^b Huqu Zhai,^b Suguru Takatsuto,^c Shogo Matsumoto,^d Shozo Fujioka,^d Kenneth A. Feldmann,^a and Roger I. Pennell^{a,1}

^aCeres Inc., Thousand Oaks, California 91320

^bInstitute of Crop Sciences, Chinese Academy of Agricultural Sciences, Beijing 100081, China

^cDepartment of Chemistry, Joetsu University of Education, Joetsu-shi, Niigata 943-8512, Japan

^dAdvanced Science Institute, RIKEN (The Institute of Physical and Chemical Research), Wako-shi, Saitama 351-0198, Japan

Genes controlling hormone levels have been used to increase grain yields in wheat (*Triticum aestivum*) and rice (*Oryza sativa*). We created transgenic rice plants expressing maize (*Zea mays*), rice, or *Arabidopsis thaliana* genes encoding sterol C-22 hydroxylases that control brassinosteroid (BR) hormone levels using a promoter that is active in only the stems, leaves, and roots. The transgenic plants produced more tillers and more seed than wild-type plants. The seed were heavier as well, especially the seed at the bases of the spikes that fill the least. These phenotypic changes brought about 15 to 44% increases in grain yield per plant relative to wild-type plants in greenhouse and field trials. Expression of the *Arabidopsis* C-22 hydroxylase in the embryos or endosperms themselves had no apparent effect on seed weight. These results suggested that BRs stimulate the flow of assimilate from the source to the sink. Microarray and photosynthesis analysis of transgenic plants revealed evidence of enhanced CO₂ assimilation, enlarged glucose pools in the flag leaves, and increased assimilation of glucose to starch in the seed. These results further suggested that BRs stimulate the flow of assimilate. Plants have not been bred directly for seed filling traits, suggesting that genes that control seed filling could be used to further increase grain yield in crop plants.

INTRODUCTION

Many of the semidwarf but high-yielding crop varieties that were developed during the Green Revolution are defective in gibberellin biosynthesis or unresponsive to gibberellin (Peng et al., 1999; Sasaki et al., 2002). Of the other plant hormones, cytokinins and brassinosteroids (BRs) seem to be among the most useful for controlling plant productivity. BR mutants can be dwarfs, and overexpression of coding sequences active in the BR biosynthesis pathway can result in higher per-plant seed yields (Choe et al., 2001).

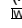
Like many hormones, BRs affect many plant processes, including those that control tiller number, leaf size, and leaf angle (Fujii et al., 1991; Sakamoto et al., 2005; Morinaka et al., 2006). This suggests that manipulation of BR levels in specific parts of crop plants could be one way to further increase grain yields. In the case of rice (*Oryza sativa*), it seems unlikely that an overall reduction in BR levels, such as those that occur in *os-dwf4-1* mutants, could result in higher per-plant grain yields, since this reduces leaf area and harvest index (Sakamoto et al., 2005). However, reduced BR levels make the leaves of rice plants more upright, allow planting at higher densities, and provide increases

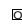
in grain yield per plot without a need for additional fertilizer (Sakamoto et al., 2005). It also seems unlikely that overall increases in BR levels, such as those that occur in plants overexpressing *DWF4* sequence, could result in higher per-plot grain yields, since this changes leaf shape, causes leaves to adopt more horizontal angles and to be more overlapping, and renders plants taller and makes them prone to lodging (Choe et al., 2001; Sakamoto and Matsuoka, 2004; Reinhardt et al., 2007). However, increased BR levels increase per-plant seed yields (Choe et al., 2001), suggesting that gain-of-function procedures need to be targeted to specific plant parts or to particular stages in development to optimize light harvesting, planting density, and grain yield.

We have been focusing on enhancing the loading of rice seed with assimilate to increase grain yield. Rice plants deficient in or insensitive to BRs produce shortened and smaller seed (Hong et al., 2005; Tanabe et al., 2005; Morinaka et al., 2006), suggesting that BRs play an important role in controlling seed size and weight. Although the mechanism for this is unclear, it has been shown that BRs can regulate the initial carboxylation activity of ribulose-1,5-bisphosphate carboxylase/oxygenase (Rubisco) and thereby influence photosynthetic CO₂ assimilation (Yu et al., 2004). Therefore, it could be that BR mutants are reduced in seed weight because of impaired transport of sucrose and other sugars to the endosperm and embryo. Alternatively, it could be that the seed are smaller because of the reduced leaf area that is available for photosynthesis (Horton, 2000) or because of reduced cell expansion in the seed themselves (Szekeeres et al., 1996; Azpiroz et al., 1998).

¹ Address correspondence to rpennell@ceres-inc.com.

The author responsible for distribution of materials integral to the findings presented in this article in accordance with the policy described in the Instructions for Authors (www.plantcell.org) is: Roger I. Pennell (rpennell@ceres-inc.com).

 Online version contains Web-only data.

 Open Access articles can be viewed online without a subscription. www.plantcell.org/cgi/doi/10.1105/tpc.107.055087

To investigate how BRs affect seed weight, we used an *S-ADENOSYLMETHIONINE SYNTHASE* promoter (pAS), which we show to be active in the stems, leaves, and roots of rice plants, but not active in the flowers other than in the filaments of the stamens or in the seed other than in the epidermis of the seed coat, to control the expression of each of four sterol C-22 hydroxylases active in BR biosynthesis in rice. These were a maize (*Zea mays*) CYP724B3 cDNA (Zm-CYP), an *Arabidopsis thaliana* CYP90B1 cDNA (At-CYP) or a corresponding genomic sequence (At-gCYP), and a rice CYP90B2 cDNA (Os-CYP). We used DNA sequences encoding sterol C-22 hydroxylases for these experiments rather than others encoding different enzymes in the BR biosynthetic pathway or BR signaling proteins because the C-22 hydroxylation of campestanol (CN) to 6-deoxocathasterone (6-DeoxoCT) is rate limiting in the pathway and effective for increasing the levels of the BRs with significant biological activity (Choe et al., 1998), which are castasterone (CS) and brassinolide (BL). We used cDNA clones from three plant species in an attempt to compare the effects of related monocot and dicot sequences on seed development in a monocot.

By manipulating the BR pathway in the stems, leaves, and roots of rice, we generated 15 to 44% increases in grain yield per plant in greenhouse- and field-grown plants containing Zm-CYP, Os-CYP, and At-gCYP transgenes relative to wild-type plants, some of which was the result of an increase in seed weight. By comparing the At-gCYP plants that differed in transgene mRNA levels and the extent of the phenotypic changes, we show that At-gCYP stimulated CO₂ uptake and the filling of the seed. These results suggest that genes controlling BR levels could be useful for increasing seed filling and grain yield in crop plants.

RESULTS

Construction of Plants Overexpressing Sterol C-22 Hydroxylase Genes

We characterized an *Arabidopsis* pAS promoter in rice. Imaging (Figures 1A to 1F) and RT-PCR analysis (Figure 1K) of green fluorescent protein (GFP) expression in rice plants carrying a two-component construct containing pAS, the yeast transcriptional activator *HAP1*, five tandem repeats of the yeast upstream activating sequence recognized by *HAP1* (*HAP1*_{UAS}), and *GFP* (pAS:*HAP1*:*UAS*_{HAP1}:*GFP* [aHAP]; see Supplemental Figure 1 online) showed that pAS directs expression to many or all of the cells in the stems, leaves, and roots of rice but not to the flowers other than weakly in the filaments of the anthers or to the seed other than weakly in the epidermis of the seed coat. In these plants, *HAP1* operated in *cis* to activate the *HAP1*_{UAS} repeats and drive amplified expression of *GFP* (Zhang and Guarente, 1994; Johnson et al., 2005). Imaging of plants containing a pAS:*GFP* direct fusion showed a similar, but weaker, expression pattern. By contrast, imaging and RT-PCR analysis of the expression of a rice *UBIQUITIN2* promoter (p*RUBQ2*:*HAP1*:*UAS*_{HAP1}:*GFP* [uHAP]; see Supplemental Figure 1 online) showed that there was *GFP* expression in the flowers and seed as well (Figures 1G, 1J, and 1K). Thus, pAS activity is widespread in developing rice plants but essentially ceases at the onset of

inflorescence development and resumes again in the next generation. Imaging showed that this was ~2 d after the start of germination (Figure 1H), with expression resuming in the shoot and root ~3 d later (Figure 1I).

We then used pAS to direct the expression of Zm-CYP724B4 (Zm-CYP), At-CYP90B1 (At-CYP), and Os-CYP90B2 (Os-CYP) cDNAs to the stems, leaves, and roots of rice. To begin, we prepared a series of direct fusions and used them to develop transgenic rice plants, so that we could compare the effects of related monocot and dicot sequences on growth and seed development. Then, we used a genomic At-CYP90B1 sequence as a direct fusion (At-gCYP) and through a series of aHAP × *UAS*_{HAP1}:At-gCYP90B1 (uAt-gCYP) two-component crosses to compare and amplify the effects of the genomic sequence originally shown to increase seed yield (Choe et al., 2001) with those of the cDNAs. In double hemizygous F1 plants arising from the crosses, *HAP1* operated in *cis* and in *trans* to activate two sets of five *UAS*_{HAP1} repeats and drive amplified expression of GFP and At-gCYP (see Supplemental Figure 1 online). For the direct fusions, we generated ~10 independent transgenic lines carrying single T-DNAs and examined ~14 T2 generation homozygous plants for each of them (we did not study the hemizygotes). For the two-component crosses, we also generated ~10 independent transgenic lines carrying single T-DNAs for each of the parents to be used for the crosses and developed ~10 T1 generation hemizygous plants for each of them; we used pollen from each of four aHAP plants to pollinate each of four uAt-gCYP plants and examined up to ~20 double hemizygous F1 plants from each of the crosses.

RT-PCR using coding sequence and terminator primers for each of the cDNAs, or spanning the boundary between the fifth and sixth exons of the At-gDNA, allowed us to identify Zm-CYP, Os-CYP, At-CYP, and At-gCYP (including uAt-gCYP) plants containing the respective mRNAs. RT-PCR also allowed us to see that the Zm-CYP, Os-CYP, At-CYP, and At-gCYP mRNAs had the predicted sizes, although in some At-gCYP lines, the pre-mRNAs were not efficiently spliced (Figure 1L) and the mRNA levels in At-CYP lines were quite variable (Figure 1M) relative to the RT-PCR products for rice β-tubulin, which were used as an internal control. Quantitative RT-PCR of Os-CYP and wild-type plants using coding sequence primers showed that the rice transgene was expressed at a level between ~15-fold (Os-CYP-6 plants, *P* = 7.73E-04) and ~25-fold (Os-CYP-15 plants, *P* = 1.40E-05) higher than that of the endogenous gene.

Accordingly, we identified seven lines for metabolite analysis and preliminary phenotypic observations, focused on three of the seven (Zm-CYP-1, Os-CYP-14, and At-gCYP-5 lines) as well as some F1 plants from aHAP₁ × uAt-gCYP crosses (aHAP-7 × uAt-gCYP-16 crosses) for phenotypic evaluations and field studies and used one of the four (At-gCYP-5) together with a line containing the same transgene but showing lower transgene mRNA levels (At-gCYP-3) for microarrays and photosynthesis experiments (Table 1). The three lines were representative of each of the transgenes phenotypically. We did not include any At-CYP plants among those grown in the field because they were phenotypically similar to the At-gCYP plants (that spliced the pre-mRNA) but tended to be more variable in transgene mRNA levels (Figure 1M).

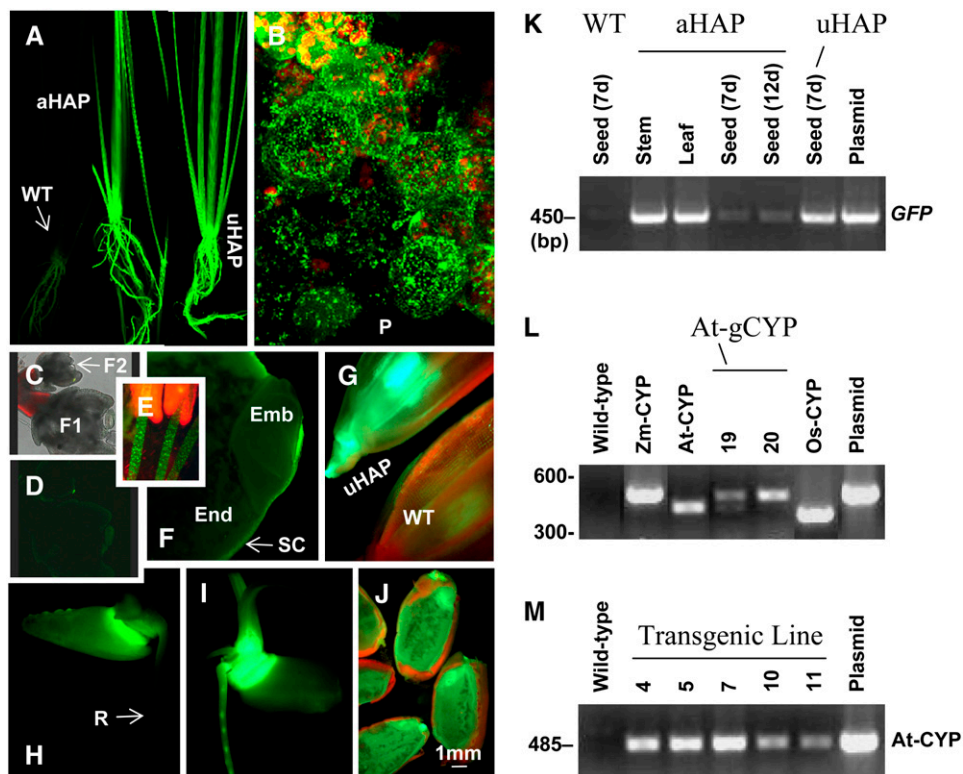


Figure 1. Expression Pattern of an *Arabidopsis* pAS Promoter in Rice.

(A) aHAP fluorescence in roots and leaves. **(B)** aHAP fluorescence in mesophyll cells. **(C)** and **(D)** aHAP in flower buds (no fluorescence). **(E)** aHAP fluorescence in filaments. **(F)** aHAP fluorescence in seed (15 d after pollination). **(G)** and **(J)** uHAP fluorescence in flowers and seed. **(H)** and **(I)** aHAP fluorescence in germinating seed. **(K)** to **(M)** mRNA levels. Primers were designed to the coding sequence and OCS terminator of each of the transgenes. Primers to the *Os-CYP* transgene were used for the wild type and did not reveal mRNA levels for the endogenous gene. The plasmid in **(L)** contained *At-gCYP* and in **(M)** contained *At-CYP*. The top *At-gCYP* bands in **(L)** are from unspliced pre-mRNA. Emb, embryo; End, endosperm; F1 and F2, flower buds; P, pith; R, root; SC, seed coat.

Enhancement of the BR Biosynthesis Pathway

CYP724B and CYP90B proteins catalyze sterol C-22 hydroxylations in the BR biosynthesis pathway, including the hydroxylation of CN to 6-DeoxoCT (Fujita et al., 2006; Sakamoto et al., 2005). Metabolite analysis of flag leaves of *Zm-CYP-1*, *Os-CYP-6* and -14, *At-CYP-4*, and *At-gCYP-3*, -5, and -7 plants showing phenotypic changes typical of elevated BR levels revealed increases in 6-DeoxoCT and downstream BR pathway intermediates (Table 2; see Supplemental Tables 1 and 2 online). The increases in 6-DeoxoCT, 22-OH-3-one, 3-*epi*-6-DeoxoCT, 6-DeoxoTE, 6-DeoxoTY, and TY levels were conspicuous and significant in least significant difference (LSD) tests when averaged across all transgenes and all biological replicates (Table 2; see Supplemental Tables 1 and 2 online). However, metabolite analysis of seed from the same plants showed that there were not any significant changes in the levels of any of the interme-

diates (Table 2; see Supplemental Tables 1 and 2 online). These data suggested that the genes encoding the sterol C-22 hydroxylases brought about increases in the levels of BR pathway intermediates downstream of 6-DeoxoCT in the flag leaves but had little or no effect in the seed.

Of the downstream intermediates, only CS and BL have significant biological activity in plants (Shimada et al., 2001). Both are present at very low levels in plant tissues and are difficult to measure accurately. Our results for CS were not significant in LSD tests, and BL levels were too low to measure (Table 2; see Supplemental Tables 1 and 2 online), so we assayed for their activities instead. CS and BL stimulate cell elongation (Fujioka et al., 1996; Szekeres et al., 1996) and provide tolerance to heat stress (Dhaubhadel et al., 2002). We found that the number of epidermal cells at the bases of the leaf blades measuring 300 to 350 μm in length was increased to $\sim 80\%$ in *At-gCYP-5* plants from $\sim 12\%$ in wild-type plants (see Supplemental Table 3 online).

Table 1. Plant Lines

Transgene	Type of Analysis				
	BR Metabolite	Greenhouse Phenotype	Field Phenotype	Microarray	Photosynthesis
Zm-CYP	1	1	1	ND	ND
Os-CYP	6, 14	14	14	ND	ND
At-CYP	4	4	ND	ND	ND
At-gCYP	3, 5, 7	5	5	3, 5	3, 5
aHAP1 × uAt-gCYP	ND	7 × 16 F1	ND	ND	ND

Seven lines were used for metabolite analysis. Four of the seven, and F1 plants from aHAP1 × uAt-gCYP crosses, were used for phenotypic evaluations. Two At-gCYP lines were used for microarray gene expression and photosynthesis experiments. The numbers are of the specific plant lines used. ND, no data.

and that the number of seedlings in which the first two leaves were killed when two-leaf seedlings were exposed to 48°C was decreased to ~9% in At-gCYP-5 plants from ~91% in wild-type plants (see Supplemental Figure 2 and Supplemental Table 4 online), suggesting that there were increased CS and BL levels in the transgenic plants.

Phenotypic Analysis of Greenhouse-Grown Plants

When grown in a greenhouse, more than half of the homozygous Zm-CYP, Os-CYP, At-CYP, and At-gCYP T2 plants and more than two-thirds of the double hemizygous F1 plants from aHAP1 × uAt-gCYP crosses showed clear phenotypic changes. For example, Zm-CYP-1, At-CYP-4, and aHAP1-7 × uAt-gCYP-16 F1 plants produced leaves that were up to ~23% longer than those of wild-type plants grown alongside them (Figures 2A and 2C, Table 3; see Supplemental Table 5 online). The internodes were also elongated and the leaf joints higher up on the tillers (Figure 2B), so that the Os-CYP-14 and At-gCYP-5 plants, for example, were ~6% and ~10% taller, respectively, than wild-type plants (Table 3; see Supplemental Table 5 online). In contrast with the upright leaves of *os-dwf4-1* and other BR mutants (Sakamoto and Matsuoka, 2004; Sakamoto et al., 2005; Morinaka et al., 2006), the leaves of the Zm-CYP-1 plants were at increased angles to the vertical so that the plants were slightly sprawling when unsupported (Figures 2C to 2E). Tiller diameter (determined for three tillers per plant) was also increased by ~18% in aHAP1-7 × uAt-gCYP-16 F1 plants (Table 3; see Supplemental Table 5 online), although there were not any increases in leaf number per tiller in any of our transgenic plants. Some transgenic plants appeared to have more tillers, larger panicles, and more seed per panicle (determined for the largest three panicles per plant) than wild-type plants, although the differences were not significant statistically (Figures 2F and 2G, Table 3; see Supplemental Table 5 online). In contrast with the small seed typical of *os-dwf11* BR mutants (Tanabe et al., 2005), the seed of Zm-CYP-1, Os-CYP-14, and At-gCYP-5 plants were larger than those of the wild-type plants. Whereas the average weight for the seed of a Zm-CYP-1 plant, for example, was ~28 mg, the average weight for the seed of a wild-type plant was ~25 mg, which is a difference of ~14% (Figures 2H to 2K, Table 3; see Supplemental Table 5 online). The seed of the transgenic plants

were more evenly sized than those of the wild-type plants as well: the standard deviations for the weights of 100 Zm-CYP-1 and 100 wild-type seed, for example, were 1.8 and 1.5, respectively. These phenotypic changes resulted in significant ~15 to 31% increases in seed yield per plant in these greenhouse-grown transgenic plants relative to wild-type plants (Table 3; see Supplemental Table 5 online).

Table 2. BR Metabolite Analysis

Intermediate	Leaf Mean		Seed Mean	
	Wild Type	Transgenic	Wild Type	Transgenic
24MC	8233	7000	1650	1900
CR	84733	84786	70250	70200
CN	1793	1590	2360	1960
6-OxoCN	28.04	27.5	35.5	37.2
22-OHCR	0.43	1.82	0.09	0.14
22-OH-3-one	1.08	2.79*	0.15	0.54
6-DeoxoCT	1.06	2.81*	0.48	0.59
3- <i>epi</i> -6-DeoxoCT	2.23	5.29*	0.045	0.16
6-DeoxoTE	0.18	0.25*	0.085	0.060
6-Deoxo3DT	1.18	1.64	0.075	0.090
6-DeoxoTY	8.96	14.03**	0.14	0.12
6-DeoxoCS	1.84	2.84	0.115	0.11
CT	ND	ND	ND	ND
TE	0.027	0.035	0.040	0.047
TY	1.47	1.75*	0.080	0.10
CS	0.68	0.83	0.080	0.096
BL	ND	ND	ND	ND

Sterol C-22 hydroxylases increase the levels of BR intermediates downstream of 6-DeoxoCT. The numbers are arithmetic mean levels calculated from all samples analyzed (Zm-CYP-1, Os-CYP-6 and -14, At-CYP-4, and At-gCYP-3, -5, and -7 samples) in ng/g fresh weight. CR, campesterol; CT, cathasterone; TE, teasterone; TY, typhasterol; 3-*epi*-6-DeoxoCT, 3-*epi*-6-deoxocathasterone; 6-DeoxoTE, 6-deoxoteasterone; 6-Deoxo3DT, 3-dehydro-6-deoxoteasterone; 6-DeoxoTY, 6-deoxytyphasterol; 6-DeoxoCS, 6-deoxocastasterone; 6-OxoCN, 6-oxocampestanol; 22-OH-3-one, (22S,24R)-22-hydroxy-5 α -ergostan-3-one; 22-OHCR, (22S)-22-hydroxycampesterol; 24-MC, 24-methylenecholesterol. ND, not detected. *, Statistically different from the wild type at 5% level; **, statistically different from the wild type at 1% level.

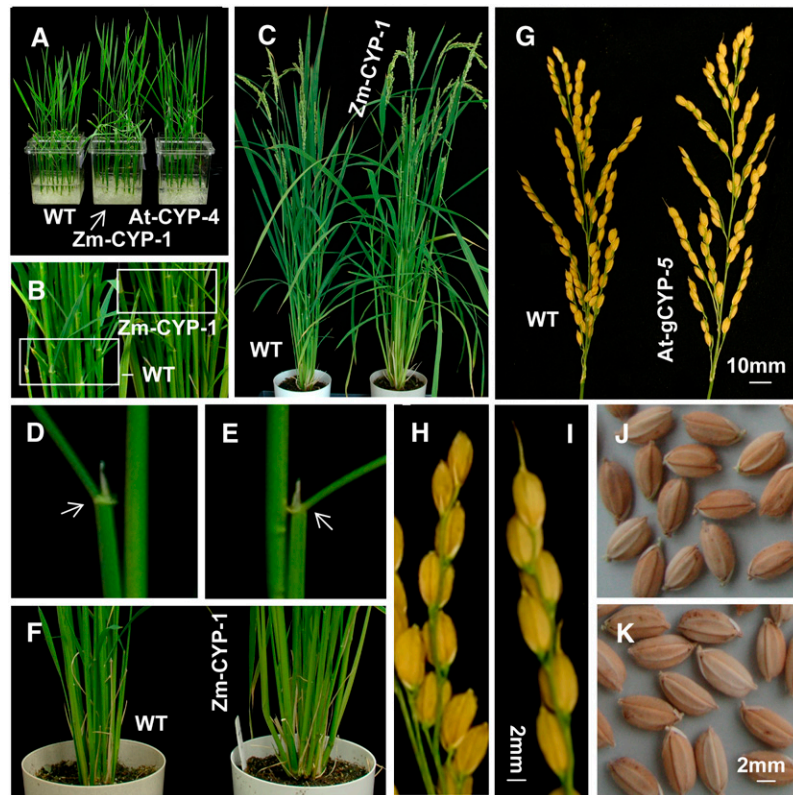


Figure 2. Greenhouse Phenotypes.

- (A) Leaf height of seedlings.
 (B) Leaf sheath. The boxes show the positions of the nodes.
 (C) Leaf angle.
 (D) Leaf angle in the wild type.
 (E) Leaf angle in Zm-CYP-1.
 (F) Tillering.
 (G) Panicle size (the panicles are among the largest three for each plant).
 (H) and (J) Seed size in the wild type (branch 9).
 (I) and (K) Seed size in Zm-CYP-1 (branch 9).
 Arrows in (D) and (E) point to leaf joints.

In contrast with these Zm-CYP-1, Os-CYP-14, and At-gCYP-5 plants that showed clear phenotypic changes, several other transgenic plants that failed to splice the transgene pre-mRNA correctly (such as At-gCYP-19 plants) or that showed low transgene mRNA levels (such as At-gCYP-3 plants) were not significantly taller than the wild-type plants and showed little or no evidence of increases in leaf angle or tiller diameter.

Since pAS is not active in the seed other than weakly in the epidermis of the seed coat, these data suggested that the increases in seed weight were secondary effects of the transgenes, resulting from BR activities elsewhere in the plant. To test this, we used an *INT:HAP1:UAS_{HAP1}:GFP* enhancer trap line (iHAP) that directs expression only to the embryo (Figure 3A; see Supplemental Figure 1 online) and a rice *GLOBULIN1* promoter (*pGLB1*) that is active only in the endosperm (Wu et al., 1998) as a *pGLB:HAP1:UAS_{HAP1}:GFP* construct (gHAP) (Figure 3A; see Supplemental Figure 1 online) to direct expression of At-gCYP

to the endosperm. This was accomplished by performing iHAP-60 × uAt-gCYP-17 and gHAP-5 × uAt-gCYP-17 two-component crosses (see Supplemental Figure 1 online). When we selfed the double hemizygous F1 plants from these crosses and sorted the F2 seed according to the level of GFP fluorescence, we found that there were three groups of seed representing those that were wild-type (GFP⁻), hemizygous (GFP⁺), and homozygous (GFP⁺⁺) for the respective *HAP1* constructs (Figures 3B and 3C). The expected segregation of the *UAS_{HAP1}:At-gCYP* construct within each group was 3:1, meaning that ~75% of the seeds in each of the GFP⁺ and GFP⁺⁺ groups should have transcribed the At-gCYP sequence and accumulated higher BR levels. However, when we examined these seed, we could not find any significant effects on their weight (Figure 3D).

These experiments further suggested that the increases in seed weight in Zm-CYP, Os-CYP, and At-gCYP plants resulted from BR activities in the stems and leaves rather than in the seed

Table 3. Phenotype Data from Greenhouse-Grown Plants

Trait	Wild Type	Zm-CYP-1	Os-CYP-14	At-gCYP
Seed yield				
Number of seed panicle ⁻¹	58.0	ND	ND	66.0 ^a
Number of seed plant ⁻¹	376	430	416	393 ^b
Weight (g) 100 seed ⁻¹	2.48	2.83 ^{**}	2.63 ^{**}	2.73 ^{**b}
Seed yield (g) plant ⁻¹	9.22	12.1 ^{**}	10.9 [*]	10.6 ^{ab}
Plant Size				
Leaf length (cm)	26.0	ND	ND	32.0 ^{*a}
Internode length (cm)	28.3	ND	ND	35.0 ^{*a}
Height (cm) plant ⁻¹	89.9	93.0	95.6 [*]	98.8 ^{**b}
Number of tillers plant ⁻¹	9.38	10.3	9.88	11.1 ^b
Tiller diameter (cm)	0.11	ND	ND	0.13 ^{*a}

Sterol C-22 hydroxylases affect development and seed weight. Tillers were counted when the plants flowered, ~2 months after germination. Stem, leaf, and seed size measurements were taken at maturity, ~3 months after germination. ND, no data. *, Statistically different from the wild type at 5% level; **, statistically different from the wild type at 1% level.

^a aHAP-7 × uAt-gCYP-16.

^b At-gCYP-5.

themselves. We examined this by weighing two sets of 100 double hemizygous F₂ seed from aHAP1-7 × uAt-gCYP-16 and aHAP1-7 × uAt-gCYP-17 crosses, ordering the weights from heaviest to lightest, and subtracting from them the weights of 100 wild-type seed, which were also ordered from heaviest to lightest. We found that the greatest increases in the weights of these seed were associated with the lightest seed (the seed that fill the least) in wild-type plants (Figure 4), which are at the base of the spikes. These results explained the more even sizes of the transgenic seed and suggested that at least some of the increase in seed weight in the Zm-CYP, Os-CYP, and At-gCYP plants resulted from enhanced seed filling, especially of the seed at the base of the spikes. The iHAP and gHAP crosses also suggested that rice embryo and endosperm tissues were unable to respond to BRs directly, although seed from some other iHAP × uAt-gCYP crosses, which resulted in very high At-gCYP mRNA levels, were delayed in germination, suggesting that there could have been an effect on embryo dormancy.

Field Experiments

When grown in paddy fields, Zm-CYP-1, Os-CYP-14, and At-gCYP-5 T₃ plants showed phenotypic changes similar to those for the greenhouse-grown plants, although the additional fertilizer applied to fields made the grain yields generally larger. For example, the Zm-CYP-1 plants produced seed that were ~19% heavier (when measured for the five largest of the 60 plants growing in each plot) than the seed of the wild-type plants (Figures 5A and 5B, Table 4; see Supplemental Table 6 online). This, in contrast with the reduced per-plant yields typical of *os-dwf4-1* BR mutants grown in fields (Sakamoto et al., 2005), resulted in ~32 to ~44% increases in grain yield per plant in the Zm-CYP-1 and Os-CYP-14 plots (Table 4; see Supplemental Table 6 online) and ~44 to ~59% increases in grain yield when

averaged across the four plots. The At-gCYP-5 plants seemed to perform better as well, although their grain yield was not statistically higher than the wild-type plants (Figure 5E, Table 4; see Supplemental Table 6 online). There were also up to 19% increases in height in the transgenic plants and up to 28% increases in tiller number in the Zm-CYP-1 and At-gCYP-5 plants, which contributed to an up to 42% increase in biomass (Figures 5C and 5D, Table 4; see Supplemental Table 6 online). Some transgenic plants appeared to have more panicles than

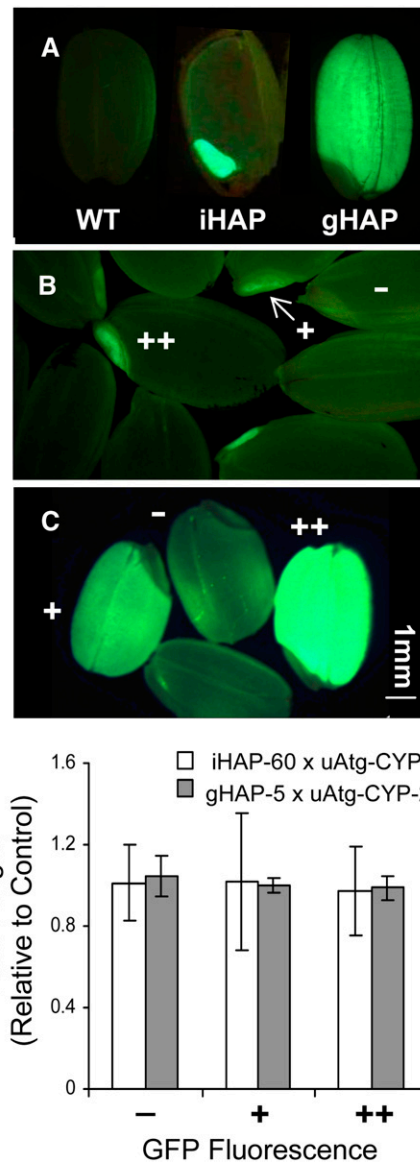


Figure 3. Expression of At-gCYP in Seed.

(A) Fluorescence in seed.

(B) iHAP × uAt-gCYP fluorescence in F₂ seed.

(C) gHAP × uAt-gCYP fluorescence in F₂ seed.

(D) Weights of F₂ seed. -, +, and ++ represent segregants: wild type, hemizygous, and homozygous for GFP. Bars indicate SE.

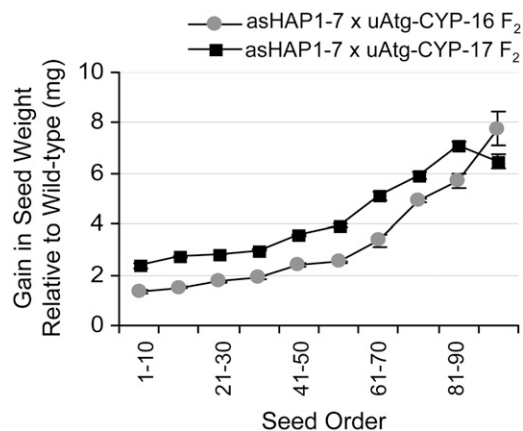


Figure 4. Effects of At-gCYP on Seed Filling.

The data were calculated by weighing two sets of 100 double hemizygous aHAP1 \times uAt-gCYP F₂ seed and 100 aHAP1 \times uAt-gCYP F₂ seed, ordering each group of weights from heaviest to lightest, and subtracting from them the weights of 100 wild-type seed. The heavier seeds are to the left and the lighter to the right. Bars indicate SE.

wild-type plants, although the differences were not statistically significant (Table 4; see Supplemental Table 6 online).

The largest and most significant grain yield increases were in our Zm-CYP-1 plots (Table 4; see Supplemental Table 6 online). RT-PCR of many Zm-CYP lines revealed consistently high transgene mRNA levels, at least when compared with our At-gCYP lines (Figures 1L, 5F, and 5G), which could have sustained high mRNA levels in the field and help to explain these larger grain yield increases.

Gene Expression Analysis

We sought to determine if the metabolic or phenotypic changes observed in the transgenic plants could be correlated with changes in gene expression. We assayed the expression of most of the genes in the rice genome using rice microarrays containing 57,381 features in an analysis that was similar to a previous study in *Arabidopsis* (Müssig et al., 2002). The RNA samples for the microarrays came from seedling leaves, flag leaves, and seed of At-gCYP-3 and At-gCYP-5 plants.

In general terms, the microarray data were similar for both sets of RNA samples, although the changes in gene expression were greater for the data from the At-gCYP-5 plants. Statistical analysis revealed the changes in gene expression in the At-gCYP-5 plants that had P values of <0.05 and fold inductions of >2 relative to wild-type plants. Only the genes in this category were studied further. Analysis of these genes showed that whereas 144 features corresponding to 53 genes were defined as induced and 760 features corresponding to 363 genes were defined as repressed in At-gCYP-5 seedling leaves (see Supplemental Data Set 1 online) and 137 features corresponding to 61 genes were defined as induced and 151 features corresponding to 71 genes were defined as repressed in At-gCYP-5 flag leaves (see Supplemental Data Set 2 online), there were 6256 features corresponding to 3988 genes defined as induced and

2775 features corresponding to 1816 genes defined as repressed in At-gCYP-5 seed (see Supplemental Data Set 3 online). Since the expression levels of the homologous genes were mostly unaltered through the course of seed development in *Arabidopsis* wild-type plants (<http://www.Arabidopsis.org/info/expression/ATGenExpress.jsp>), we concluded that these changes were brought about by the At-gCYP transgene. The most conspicuous result for any single gene was the ~19-fold induction of a Gly-rich cell wall protein (Os07g32710) in all four of the At-gCYP-5 seedling and flag leaf samples (see Supplemental Table 7 online), which could have been associated with cell expansion in the growing basal parts of the developing leaves (Xu et al., 1995).

By filtering the 132 regulated flag leaf genes for those that carried COG_PFM (http://www.ncbi.nlm.nih.gov/COG/) functional category descriptions, we identified a group of 32 genes with such descriptions. Of these, 15 were involved with transcription, seven in DNA replication, recombination, and repair, and six with posttranslational modification, protein turnover, and chaperone functions. By clustering the features on the chip with P values of <0.05 and fold inductions of >2, we identified a group of 33 genes that were expressed only in the flag leaves of wild-type plants and induced only in the flag leaves of At-gCYP-5 plants (Figure 6A). These 33 genes included 17 protein kinases (Os01g02780, Os01g02790, Os01g02810, Os01g41750, Os02g13420, Os02g13460, Os04g30030, Os04g34250, Os05g13770, Os05g44570, Os07g03880, Os07g35010, Os09g09510, Os09g16950, Os09g29540, Os10g40490, and Os12g17550) and a *BRI1*-associated receptor kinase precursor (Os11g31530) encoding a protein 38% identical to *Arabidopsis BRI1* (which is repressed by BRs; Nemhauser et al., 2004) but 52% identical to *Arabidopsis BAK1*, suggesting that BRs exert complex feedback control over the BRI1/BAK1 heterodimer (Nam and Li, 2002).

By filtering the 5804 regulated seed genes in the same way, we identified a group of 1185 genes. Of these, 308 were involved with transcription, 300 had a general function prediction only, 206 were involved with DNA replication, recombination, and repair, 152 with amino acid transport and metabolism, 148 with carbohydrate transport and metabolism, 119 with translation, ribosomal structure, and biogenesis, and 107 with inorganic ion transport and metabolism. By clustering the features on the chip with P values of <0.05 and fold inductions of >2, we identified a group of 28 genes that were expressed only in the seed of wild-type plants and induced only in the seed of At-gCYP-5 plants (Figure 6A). These 28 genes included 12 hypothetical proteins (Os02g15140, Os02g41610, Os02g56500, Os04g31170, Os04g38270, Os04g44580, Os08g40350, Os09g20340, Os10g25180, Os10g40260, Os11g06410, and Os11g38610) and a homolog of *FIE* (Os08g04290), which in *Arabidopsis* is known to be induced by vernalization (Wood et al., 2006) but not by BRs. It was interesting that the kinases were not only expressed at higher levels in flag leaves than in seed but also at higher levels than in seedling leaves (Figure 6A).

When we checked >30 metabolic pathways in the KEGG metabolic pathway database (<http://www.genome.jp/kegg/pathway.html>), we found three pathways in which consecutive genes in entire pathway branches were defined as induced or defined as

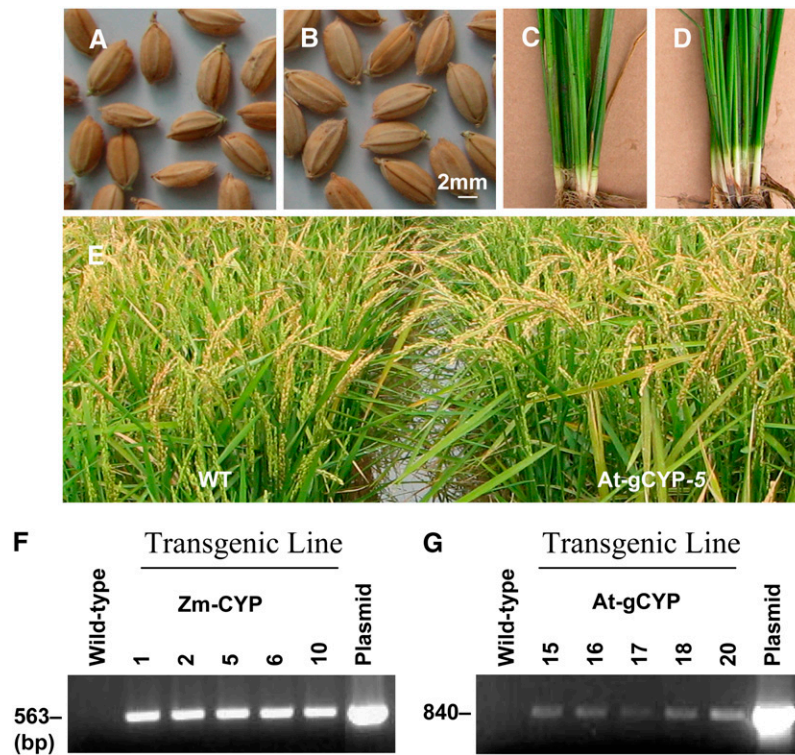


Figure 5. Field Phenotypes.

(A) Seed size in the wild type.

(B) Seed size in Zm-CYP-1.

(C) Tiller number in the wild type.

(D) Tiller number in Zm-CYP-1.

(E) Mature plants in the field.

(F) and (G) Representative RT-PCR of mRNA levels. The RT-PCR primers in (F) were the same as those for Zm-CYP in Figure 1L, but the primers in (G) were different from those for At-gCYP in Figure 1L. All primers were designed to coding and terminator sequences.

repressed. These were the pathways representing the shunt from glucose-1-phosphate to trehalose in the flag leaf, the pathway from glucose-6-phosphate to sucrose and starch in the seed, and the pathway from geranyl pyrophosphate to cycloartenol and lanosterol in the seed (see Supplemental Table 8 online).

We examined all 15 genes in the three pathway branches by quantitative RT-PCR (qRT-PCR), using mRNAs from At-gCYP-5 flag leaf and seed samples for the reactions, and found that the microarray and qRT-PCR results were in general agreement given the kind of quantitative differences that are typical when the two procedures are compared (Wang et al., 2003; Misson et al., 2005) (see Supplemental Table 8 online). Specifically, according to this qRT-PCR, there was an approximately 2- to 5-fold repression of UDP-glucose pyrophosphorylase (UGPase) (Os02g02560), trehalose-phosphate synthase (Os05g44100), and trehalose phosphatase (Os02g54820) at consecutive steps in the shunt from glucose-1-phosphate to trehalose in all four of the flag leaf samples (Figure 6B; see Supplemental Table 8 online). There was an ~13-fold to ~720-fold induction of phos-

phoglucomutase (Os10g11140), UGPase, sucrose-phosphate synthase (Os06g43630), sucrose synthase (Os03g22120), glucose-1-phosphate adenyltransferase (Os05g50380), starch synthase (Os05g45720), and 1,4- α -glucan branching enzyme (Os02g32660) at consecutive steps in the pathway from glucose-6-phosphate to sucrose and starch in all eight of the seed samples, according to qRT-PCR and classified according to KEGG (Figure 6C; see Supplemental Table 8 online). There was an ~7-fold to ~30-fold induction of farnesyl-diphosphate synthase (geranyltransferase) (Os05g46580), geranylgeranyl-pyrophosphate synthase (Os07g39270), squalene synthase (Os03g59040), squalene monooxygenase (Os03g12900), cycloartenol synthase (Os11g18366), and lanosterol synthase (Os02g04710) at consecutive steps in the pathway from geranyl pyrophosphate and geranylgeranyl pyrophosphate synthase to cycloartenol (Bouvier-Navé et al., 1998) and lanosterol (Jiang and Wang, 2006) in all eight of the seed samples, also according to qRT-PCR and classified according to KEGG (Figure 6D; see Supplemental Table 8 online). These results showed that all three pathways were tightly controlled by BRs.

Table 4. Phenotype Data from Field-Grown Plants

Trait	Wild Type	Zm-CYP-1	Os-CYP-14	At-gCYP-5
Grain Yield				
Number of panicles plant ⁻¹	16.8	23.1	21.0	20.6
Weight (g) 100 seed ⁻¹	2.37	2.83**	2.56**	2.82**
Grain Yield (g) plant ⁻¹	13.6	19.6**	17.9*	16.3
Grain Yield (g) plant ⁻¹ day ⁻¹	0.44	0.58	0.53	0.53
Grain Yield (g) plot ⁻¹	537	853**	774*	603
Grain Yield (g) plot ⁻¹ day ⁻¹	17.3	25.08	22.80	19.46
Plant Size				
Height (cm) plant ⁻¹	61.1	71.6**	72.6**	71.0**
Height (cm) plant ⁻¹ day ⁻¹	1.97	2.10	2.14	2.29
Number of tillers plant ⁻¹	9.70	12.5**	10.9	12.4**
Biomass (g) plant ⁻¹	26.7	37.9**	35.7**	33.3*
Biomass (g) plant ⁻¹ day ⁻¹	0.86	1.11	1.04	1.08

Sterol C-22 hydroxylases affect growth and development and seed weight in paddy fields. Tillers were counted 20 d after transplanting to paddy fields, whereas panicles were counted at maturity, ~2.5 months later. More tillers were produced in between 20 d after transplanting and maturity, and most of the tillers went on to produce a single panicle. Grain yield per plant was measured for five of the plants growing in each of the plots, and grain yield, plant height, and biomass per plant were divided by the number of days from transplanting to the time when the plants flowered, ~2 months after germination, to give productivity per day. *, Statistically different from the wild type at 5% level; **, statistically different from the wild type at 1% level.

Photosynthesis

Our flag leaf and seed gene expression data and our seed weight studies suggested that the effects of the Zm-CYP, Os-CYP, and At-gCYP transgenes on seed weight were indirect and resulted from greater loading of sucrose and other sugars to the phloem and enhanced transport to the endosperm in the seed. We therefore studied photosynthesis itself to examine the possibility that there was greater sucrose accumulation in the leaves.

The maximum quantum efficiency (F_v/F_m) of the At-gCYP plants was increased by up to ~2.5% in 150 and 1100 $\mu\text{mol m}^{-2} \text{s}^{-1}$ of white light (Figure 7A) and CO_2 uptake was increased by up to ~30% at 380 ppm CO_2 and by up to 45% at 760 ppm CO_2 in higher intensities in the range from 0 to 2000 $\mu\text{mol m}^{-2} \text{s}^{-1}$ of white light (Figure 7B) relative to wild-type plants. However, At-gCYP-3 plants, which contained lower transgene mRNA levels, showed increased F_v/F_m in only 1100 $\mu\text{mol m}^{-2} \text{s}^{-1}$ light conditions and lesser (although statistically significant) increases in CO_2 uptake (Figures 7A and 7B), even though some of the BR pathway intermediates downstream of 6-DeoxoCT were increased in more or less the same way in one of the two At-gCYP-3 flag leaf replicates (see Supplemental Tables 1 and 2 online).

According to the microarrays, there were very few gene expression changes in the flag leaves of the At-gCYP-5 plants

that could have been associated with enhanced photosynthesis. Of the 108 annotated genes represented on the chips that encoded proteins affecting the reaction centers or CO_2 assimilation, there was only an ~1.4-fold induction of a Rubisco small subunit (Os12g19470) and an ~3-fold repression of a light-regulated U-box ubiquitin ligase (Os04g34140) in each of the four flag leaf samples, which qRT-PCR showed to be ~2.5-fold induced and ~6.2-fold repressed, respectively (see Supplemental Table 9 online). There was also microarray evidence for an ~2.6-fold repression of a chloroplast protease (Os06g12370) in the At-gCYP-5 flag leaves, although the qRT-PCR data, which suggested that the repression was ~2.3-fold, were not significant statistically (see Supplemental Table 9 online). However, overexpression of an *Arabidopsis* gene (At2g30950) encoding a protein 64% identical to this protease, in *Arabidopsis*, resulted in albinos at the five-leaf stage (see Supplemental Figure 3 online), suggesting that genes encoding proteins of this kind could have played a role in controlling photosynthesis (García-Lorenzo et al., 2005; Sjögren et al., 2006).

DISCUSSION

Increased BR Levels Affect Development and Increase Seed Weight

We introduced DNA sequences encoding three sterol C-22 hydroxylase proteins sufficient to catalyze key reactions in the BR biosynthesis pathway (Sakamoto et al., 2005) into rice plants. These coding sequences resulted in increases in BR levels, tiller and seed number per plant, and seed weight, especially of the seed that are normally the lightest. They also resulted in increases in leaf length and angle, height, and tiller diameter. All these traits can be valuable in rice and other crop species.

Elevated BR levels increase branch number in *Arabidopsis* and tobacco (*Nicotiana tabacum*; Choe et al., 2001) and also increase tiller number in rice, even though the branches develop from the axils on the main stem and the tillers from bases of the culms (Doust, 2007). This suggests that the processes that determine branching and tillering are conserved in dicots and monocots and that BRs help to control the processes in them both. Several genes that influence tillering in monocots have been identified, such as *MONOCULUM1* (Li et al., 2003), *TEOSINTE BRANCHED1* (Takeda et al., 2003), and *HIGH-TILLERING DWARF1* (*HTD1*; Zou et al., 2005), but a link between the activity of these genes and BR levels has not been demonstrated. However, auxin affects the expression of *HTD1* (Zou et al., 2005, 2006), and BRs interact with auxin (Nemhauser et al., 2004, 2006), suggesting that auxin could provide this link.

We show that BR levels that are elevated in the leaves, and probably also elevated in the stems and roots, have significant effects on the weight of the seed. BRs do not undergo long-distance transport in pea (*Pisum sativum*; Symons and Reid, 2004), and small amounts of radiolabeled BRs applied to the leaves of rice do not enter the seed (Yokota et al., 1992), suggesting that these increases in weight were secondary effects resulting from BR effects elsewhere in the plant. Our BR metabolite analysis that showed that there were not any significant changes in any of the pathway intermediates in the seed of

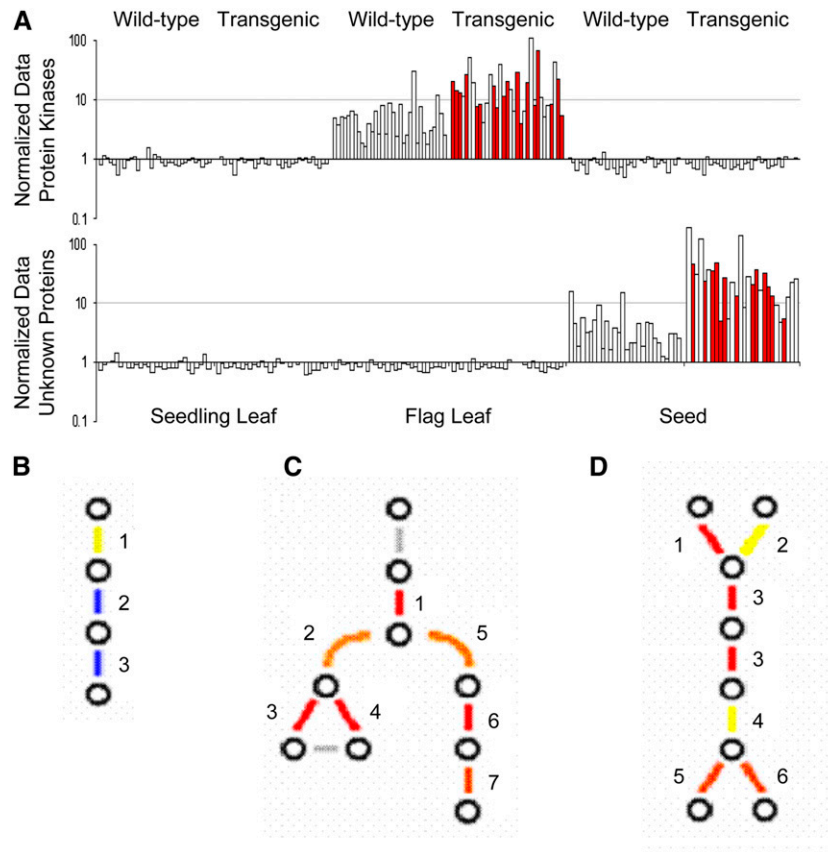


Figure 6. Microarray Gene Expression Analysis.

(A) Induction of the 33 genes expressed only in the flag leaf, including 18 genes encoding protein kinases (red), and induction of the 28 genes expressed only in the seed, including 12 genes encoding hypothetical proteins (red).

(B) Microarray data represented as colored lines for UDP-glucose pyrophosphorylase (1), trehalose-phosphate synthase (2), and trehalose phosphatase (3) in the shunt from glucose-1-phosphate to trehalose in the flag leaf.

(C) Microarray data represented as colored lines for phosphoglucomutase (1), UGPase (2), sucrose-phosphate synthase (3), sucrose synthase (4), glucose-1-phosphate adenylyltransferase (5), starch synthase (6), and 1,4- α -glucan branching enzyme (7) in the pathway from glucose-6-phosphate to sucrose and starch.

(D) Microarray data for farnesyl-diphosphate synthase (1), geranylgeranyl-pyrophosphate synthase (2), squalene synthase (3), squalene mono-oxygenase (4), cycloartenol synthase (5), and lanosterol synthase (6) in the pathway from geranyl pyrophosphate and geranylgeranyl-pyrophosphate to cycloartenol and lanosterol in the seed.

Orange and red, >2-fold and >5-fold induction, respectively; blue, >2-fold repression; yellow, no change; gray, no data.

the Zm-CYP, Os-CYP, and At-gCYP plants and our targeting of At-gCYP expression to the embryo and endosperm that showed that BRs cannot bring about seed enlargement directly also suggest that this is the case. Our ordered seed weight measurements suggest instead that the increases in seed weight resulted from enhanced filling of the seed with sucrose and other sugars transported to them from the leaves. Spray application of epibrassinolide to sorghum plants at the heading and grain filling stages has been reported to have similar effects (Xu, 2007). However, it is also possible that the weak pAS activity in the seed coat also had an effect on the weight (Schruff et al., 2006). Since there has been little breeding for increased seed filling (Smith and Nelson, 1986), genes that control the filling could be useful for increasing seed yield.

Increased BR Levels Favor Sucrose Accumulation in the Leaf and Starch in the Seed

Seed filling depends on the flow of sucrose and other sugars from the stems and leaves to the embryo and endosperm. This flow is determined by the amount of CO₂ assimilation in the leaves, the loading of the phloem with sucrose and other sugars that can be transported, and by the activities of the enzymes that convert the sugars to starch in the seed.

CO₂ assimilation is determined by electron transport efficiency in the photosynthetic reaction centers and the carboxylation rate of Rubisco. Spray applications of BRs have been shown to affect both of these processes, increasing the quantum yield of electron transport in the photosystem II reaction centers and the

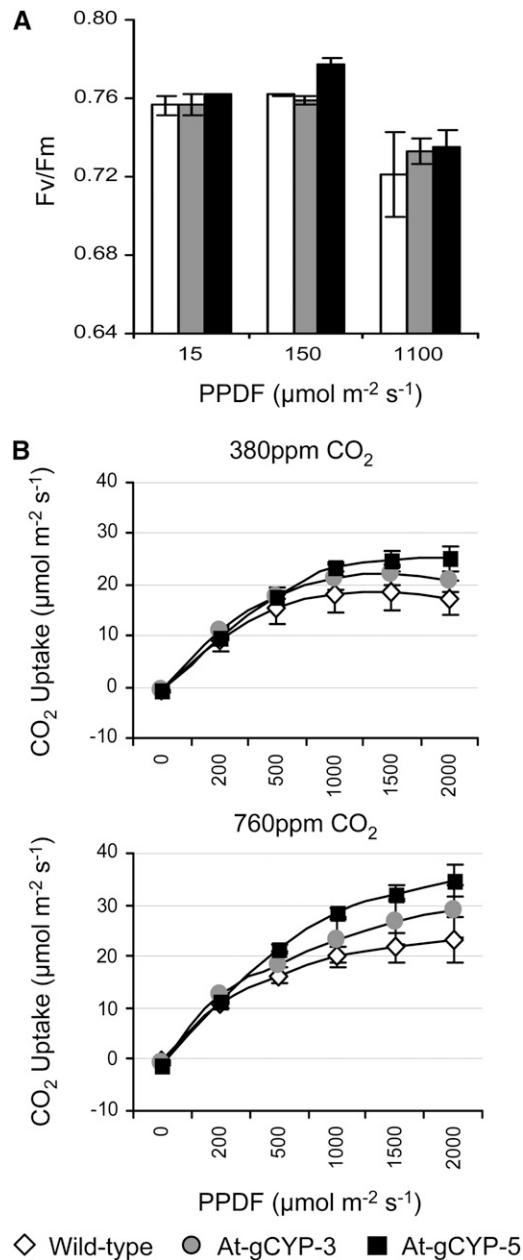


Figure 7. Effects of At-gCYP on Photosynthesis.

(A) Maximum quantum efficiency (F_v/F_m).

(B) CO_2 uptake.

Bars indicate SE.

maximum carboxylation rate of Rubisco (Fujii et al., 1991; Ramraj et al., 1997; Yu et al., 2004), and our results suggest that BR levels that are elevated by transgenes can have similar effects. Although it is not clear how BRs bring about these effects on photosynthesis, the repression of the U-box ubiquitin ligase (and the possible repression of the chloroplast protease) that were conspicuous in the microarray data might have prolonged the half-lives of some of the photosynthetic proteins, and the induc-

tion of the Rubisco small subunit might have increased the capacity for carboxylation and the accumulation of sucrose.

The loading of the phloem is determined by the activities of stem and leaf cell sugar transporters, which themselves are controlled by the levels of free sucrose and other sugars in the cytoplasm (Bürkle et al., 1998; Scofield et al., 2007). The repression of the shunt from glucose-1-phosphate to trehalose in the flag leaves of the At-gCYP plants could have affected these levels. Trehalose stimulates the expression of ADP-glucose pyrophosphorylase and starch synthesis in *Arabidopsis* (Wingler et al., 2000; Fritzius et al., 2001; Kolbe et al., 2005), so the repression of trehalose-phosphate synthase and trehalose phosphatase, which lie at consecutive steps in the shunt from glucose-1-phosphate to trehalose, in the flag leaves of the At-gCYP plants would have favored free sucrose accumulation at the expense of starch.

The accumulation of starch in the seed is determined by the activity of starch synthase and 1,4- α -glucan branching enzyme in the endosperm (Sato et al., 2003; Ryoo et al., 2007). Induction of the pathway from glucose-6-phosphate to sucrose and starch in the seed of the At-gCYP plants likely enhanced these activities and contributed to the increase in seed weight. Interestingly, UGPase was induced in the seed in these At-gCYP plants, but it was repressed in the leaf. UGPase catalyzes the reversible formation of UDP-glucose from glucose-1-phosphate and UTP, and in the seed provides UDP-glucose to starch synthase directly (Smidansky et al., 2002; Kleczkowski et al., 2004), but in the leaf provides UDP-glucose to sucrose phosphate synthetase (Kleczkowski et al., 2004). UDP-glucose is also an important intermediate in an array of metabolic pathways, including those involved in hemicellulose and pectin formation (Johansson et al., 2002). These observations suggest that regulation of UGPase in particular might play a key role in source-sink interactions in plants.

Comparison of the Effects of Maize, Rice, and *Arabidopsis* C-22 Hydroxylase Genes on Development and Seed Weight

The *Arabidopsis* At-CYP90B1 and rice Os-CYP90B2 genes encode orthologous proteins that are 71% identical and able to catalyze the C-22 hydroxylation of CN to 6-DeoxoCT in the BR biosynthesis pathway (Choe et al., 1998; Tanabe et al., 2005). The maize sequence encodes the protein Zm-CYP, which is 90% identical to CYP724B1 (Os04g39430, Gl:68565169) but only 42% identical to Os-CYP (Os03g12660, Os-CYP, Gl:60677681), suggesting that the maize gene is orthologous to Os-DWF11. Rice *os-dwf11* mutants show dwarfism and reduced seed length and seed size phenotypes that can be rescued with 6-deoxytyphasterol and typhasterol, suggesting that DWF11 proteins act downstream of DWF4 proteins (Tanabe et al., 2005). Our experiments also show that overexpression of Zm-CYP decreases CN and increases 6-DeoxoCT levels, suggesting that the At-CYP and Zm-CYP proteins can catalyze the same hydroxylation of CN to 6-DeoxoCT. Although our use of pAS to direct the expression of Zm-CYP, At-CYP, At-gCYP, and Os-CYP resulted in a characteristic set of growth and development phenotypes that were essentially indistinguishable from one another, the higher mRNA levels, higher 6-DeoxoCT levels, and slightly stronger phenotypes we observed for Zm-CYP could have been due to nucleotide sequence differences that protected the maize

pre-mRNA from RNA interference. Alternatively, they could have been due to greater effects on 22-OH-3-one and 6-DeoxoCT levels, which represent the early C-22 oxidation pathway that also leads to BR biosynthesis (Fujioka et al., 2002; Fujioka and Yokota, 2003).

Manipulation of the BR Pathway Could Increase Planting Density, Panicle Number, Light Capture, and Seed Filling in Crop Plants

We show that BRs regulate seed filling in rice. However, the relative contributions of the altered leaf architecture, increased photosynthetic efficiency, and effects on sugar metabolism in leaves and seed are difficult to determine. Our transgenic plants bore leaf blades at increased angles to the vertical relative to wild-type plants, were taller, and were slightly sprawling, and these phenotypic changes might all have contributed to the increases in seed weight.

Increases in leaf angle can expose leaf blades to more light, but because of shading can result in decreased light capture for the canopy as a whole (Sakamoto and Matsuoka, 2004). Increases in overall height might be expected to also expose leaves to more light, but *os-dwf4-1* mutants that are smaller than wild-type plants show enhanced grain yields under conditions of dense planting even without the use of additional fertilizer (Sakamoto et al., 2005), suggesting that height is not a determining factor for yield. It may therefore be that photosynthetic efficiency and the levels of free sucrose and fine control over the metabolic pathways leading to glucose, sucrose, and starch in the leaves and seed are the more important determinants of seed filling and weight.

Idealized crops require optimization for size, stem and leaf angle, and photosynthetic efficiency (Sakamoto and Matsuoka, 2004). It is possible that improvements can be made in rice and other crops by targeting BR phenotypes to different parts of plants or by developing combinations of BR phenotypes and other phenotypes as well. For example, in rice, increases in BR levels in the leaves to maximize photosynthetic efficiency and sugar conversions to glucose and sucrose, together with decreases in BR levels at the leaf joint to maximize planting density (Sakamoto et al., 2005) and targeted changes in auxin levels to increase the numbers of leaves and buds on the stems (Bainbridge et al., 2008) and in cytokinin levels to delay senescence (Smart et al., 1991; Ashikari et al., 2005), could have synergistic effects on grain productivity.

METHODS

Promoters

We used 1954 nucleotides immediately upstream of the transcription start site of the *Arabidopsis thaliana* AS gene (At3g17390, Gl:23397143) for most of our experiments. To direct expression to the embryo, we used the leader sequence and first intron of rice (*Oryza sativa*) *UBIQUITIN2* (Os02g06640, Gl:52076878) upstream of a promoterless *HAP1:UAS_{HAP1}:GFP* construct to develop an enhancer trap population (Laplace et al., 2005), within which we identified an embryo trap line giving expression only in the embryo (iHAP). In this construct, *HAP1* served as a transcriptional activator (Zhang and Guarente, 1994) able to induce and amplify the

expression downstream of *UAS_{HAP1}*. To direct expression to the endosperm, we used 976 nucleotides immediately upstream of the transcription start site of rice *GLOBULIN1* (Os05g41970, Gl:115465852), which gives expression in the endosperm (Wu et al., 1998), to develop a *pGLB:HAP1:UAS_{HAP1}:GFP* construct (gHAP). We used 2723 nucleotides immediately upstream of the transcription start site of rice *UBIQUITIN2* (Wang et al., 2000) to develop a *pRUBQ2:HAP1:UAS_{HAP1}:GFP* construct (uHAP) and give constitutive expression. Fluorescence was analyzed with a Typhoon scanner (Amersham Biosciences) and a TCS SP2 confocal microscope fitted with a 515- to 545-nm filter (Leica Microsystems). For promoter RT-PCR studies, mRNAs were extracted from stem, leaf, and seed (minus seed coat) tissues. Primers were designed to give 450-bp PCR products.

Coding Sequences

We used sequences encoding the maize (*Zea mays*), *Arabidopsis*, and rice sterol C-22 hydroxylase proteins CYP724B3 (GenBank/EMBL ESTs CA832360, CA832231, and CD438350), CYP90B1 (At3g50660, Gl:19699122), and CYP90B2 (Os03g12660, Gl:60677681), respectively, as full-length cDNAs for most of our experiments. We cloned these sequences from a maize hybrid, *Arabidopsis* ecotype Wassilewskija, and rice *japonica* variety Kitaake, respectively. We also used CYP90B1 as a genomic clone representing the start codon through 688 nucleotides downstream of the stop codon and lacking any part of the CYP90B1 promoter.

Constructs

For direct fusions, we introduced pAS and the maize, rice, and *Arabidopsis* coding sequences into a binary vector (pNB4) that was derived from pMOG800 (Knoester et al., 1998), in between promoter and OCS terminator sequences and upstream of selectable marker sequences, generating Zm-CYP, Os-CYP, At-CYP, and At-gCYP. To enable some two-component crosses, we used aHAP, iHAP, and gHAP and a separate set of constructs in which five tandem repeats of *UAS_{HAP1}* were introduced upstream of sequences encoding yellow fluorescent protein (YFP) targeted to the nucleus by a localization sequence from the histone H2B (uYFP) (Boisnard-Lorig et al., 2001) or At-gCYP (uAt-gCYP), also in pNB4.

Transformation and Expression Analysis

For transformation, we induced calli from mature Kitaake seeds and transformed calli with an *Agrobacterium tumefaciens*-mediated transformation method (Hiei et al., 1994). We generated between 10 and 16 independent T0 plants for each of the direct fusions and two-component constructs, used PCR to confirm them, and used segregation analysis to identify those containing single T-DNAs. We selfed the plants containing the single T-DNAs to generate hemizygous T1 (2nd generation) lines for two-component crosses and homozygous T2 and T3 direct fusion lines for phenotype analysis. For the enhancer trap screening, we generated ~500 independent iHAP transformants and used GFP analysis, PCR, and segregation analysis to develop a hemizygous T1 line for iHAP. For RT-PCR studies, Zm-CYP, Os-CYP, At-CYP, and At-gCYP mRNAs were extracted from leaf tissue. Primers were designed to the coding sequence and the OCS terminator of each of the transgenes to give 300- to 840-bp products; the primers to Os-CYP did not amplify the Os-CYP mRNA extracted from wild-type plants, so we used other primers both within the coding sequence to determine the expression level of this endogenous gene.

Two-Component Crosses

We used aHAP1 plants to pollinate uYFP plants (Johnson et al., 2005) and observed fluorescence color and cellular localization in the F1 to test our

two-component system. Then we used aHAP1, iHAP1, or gHAP plants to pollinate three groups of four hemizygous uAt-gCYP plants and phenotyped between 16 and 22 of the double hemizygous F1 plants from each of the crosses.

Greenhouse Data

We grew homozygous Zm-CYP, Os-CYP, At-CYP, and At-gCYP (including Zm-CYP-1, Os-CYP-14, At-CYP-4, and At-gCYP-5) T2 plants, and double hemizygous T2 plants containing aHAP (including aHAP1-7) and uAt-gCYP (including uAt-gCYP-16 and uAt-gCYP-17) alongside untransformed and wild-type segregant control plants in pots, for phenotyping. We added fertilizer to the soil preparation to begin with, bottom-watered with measured volumes of water, and grew the plants in a greenhouse in 16 h ~28°C days and 8 h ~22°C nights. We counted the number of tillers for each plant, took stem and leaf measurements from each of three tillers per plant, and determined seed number, size, and weight for each plant at maturity, which was ~3 months after germination. We determined seed number per panicle for three panicles per plant at maturity, took seed size measurements using WinSeedle software (Regent Instruments), which projects total seed area, and took seed weight measurements after drying mature seed at 42°C for 1 week.

Seed Filling Data

For filling experiments, we sorted F2 seed from iHAP-60 × uAt-gCYP-17 crosses and from gHAP-5 × uAt-gCYP-17 crosses according to the level of GFP fluorescence; there were three groups that were wild-type, hemizygous, and homozygous for GFP. Then we weighed the three groups and normalized the weights against the corresponding weights of seed from the iHAP and gHAP parent plants. We also weighed 100 F2 seed from each of two aHAP × uAt-CYP crosses aimed at expressing At-gCYP in the stems, leaves, and roots (aHAP-7 × uAt-gCYP-16 and aHAP-7 × uAt-gCYP-17 crosses), ordered the weights from heaviest to lightest, and subtracted from them the weights of 100 wild-type seed ordered in the same way to show which of the seeds gained in weight the most.

Field Data

We grew homozygous Zm-CYP-1, Os-CYP-14, and At-gCYP-5 T3 plants and untransformed wild-type control plants at the Institute of Crop Sciences field station in Changping, China, from May through October, 2005. We grew each line as four replicates in paddy fields laid out in a randomized complete block design, with plots of 60 plants arranged in four rows of 15 plants each. The distance between the plants in a row was 13.5 cm, and the distance between rows was 25 cm. For fertilizer, we added ammonium phosphate and potassium chloride at 121 kg acre⁻¹ when the plants were transplanted to the field and urea at 90 kg acre⁻¹ 5 d later at 60 kg acre⁻¹ at the onset of tillering and at 75 kg acre⁻¹ at booting. We kept the plants in 2 to 4 inches of water throughout the growing period. We determined tiller number for all plants in each plot at 20 d after transplanting, but we took other measurements for five plants in each plot at maturity, ~2.5 months after transplanting; the biomass and seed weight measurements were done after harvesting and drying mature plants and seed at 42°C for 1 week. We used LSD tests to compare transgenic plants with controls.

BR Metabolite Analysis

We determined levels of BR pathway intermediates using gas chromatography and mass spectroscopy. We collected ~30 g of flag leaves 12 d after the initiation of flowering and ~20 g of seed 15 d after pollination

from Zm-CYP-1, Os-CYP-6 and -14, At-CYP-4, At-gCYP-3, -5, and -7, and wild-type plants, growing in a greenhouse, all within 30 min of each other. Then we lyophilized them, extracted them twice with 250 mL of 4:1 methanol:CHCl₃, and purified and quantified the sterols and BRs according to methods described elsewhere (Noguchi et al., 1999; Fujioka et al., 2002). We used all data from all of the samples for statistical analysis. We assayed for BRs with biological activity by measuring 25 adaxial leaf epidermis cells at three sites at the bases of the leaves in single Zm-CYP-1 and At-gCYP-5 plants and by transferring 7-d-old seedlings containing two open leaves from 28 to 48°C for 6.5 h, returning them to the 28°C, and counting the number of first and second leaves that were killed by the 48°C treatment 7 d later.

Microarrays

For microarray experiments, we hybridized 18 chips. There were three sample types (seedling leaves 15 d after germination, flag leaves 12 d after the initiation of flowering, and seeds 15 d after pollination), three genotypes (At-gCYP-3, At-gCYP-5, and wild-type plants), and two biological replicates per genotype, each containing a pool of tissues from three different plants. We ground the samples in liquid N₂, extracted the mRNA, and hybridized the corresponding cDNAs to rice GeneChip microarrays (Affymetrix) containing 57,381 features. We then washed the chips, scanned them to generate TIFF files, and extracted them using quality scores describing spot morphology, intensity, and dye saturation. After RMA normalization using R/Bioconductor, we loaded the CEL files into GeneSpring GX (Agilent) and performed per-gene and per-chip normalizations such that expression levels for each gene on each chip were centered at ~1. We calculated biological replicate correlations by Condition Tree clustering; the correlation coefficients ranged from 0.9849 to 0.9973. We used a linear model (Smyth et al., 2005) to estimate real biological variation in gene expression levels and created a corrected signal for each of the features on each of the chips. We then used analysis of variance tests to identify the gene expression levels that were statistically different between the transgenic and wild-type plants (the general linear model for the factorial analysis of variance design with two independent variables was $U_{ijk} = \mu + t_i + \beta_j + g_{ij} + e_{ijk}$, where in our case, $U_{ijk} = \mu$ [overall mean response] + group effect #1 [t_i , transgene] + group effect #2 [β_j , tissue] + interaction term [g_{ij} , transgene:tissue] + error [e_{ijk}]) and false discovery rate correction (Benjamini and Hochberg, 1995) to control for multiple testing errors. These procedures provided us with transgenic seedling leaf to wild-type seedling leaf, transgenic flag leaf to wild-type flag leaf, and transgenic seed to wild-type seed comparisons, which allowed us to interpret the baseline expression in the wild type and the differential expression in the At-gCYP plants. Using only the expression levels that showed statistically significant changes (that had P values of < 0.05), we then identified the genes that were >2-fold induced or repressed, grouped the corresponding genes into COG_PFAM categories (<http://www.ncbi.nlm.nih.gov/COG/>), and analyzed them for enrichment against all the genes represented on the chip. We determined the statistical significance of this enrichment using χ^2 and two-tailed Yates correction values.

qRT-PCR

For confirmation of microarray results, we synthesized cDNAs from At-gCYP-3, At-gCYP-5, and wild-type flag leaf and seed mRNAs extracted from pools of flag leaves and seeds collected from three different plants per genotype and developed primers to give 75- to 150-bp PCR products. We amplified PCR products in triplicate using iQ SYBR Green SuperMix (Bio-Rad) in 15- μ L qRT-PCR reactions, an iCycler iQ 96-well real-time PCR detection system (Bio-Rad), iCycler software to calculate threshold cycle values, and rice β -tubulin as an internal control. We used the 2^{- $\Delta\Delta C_T$} method to calculate the relative expression levels for the At-gCYP-5 and

wild-type samples and a two-tailed *t* test to compare the ratios and determine statistical significance (Livak and Schmittgen, 2001). We placed qRT-PCR-validated genes into pathways using the KEGG metabolic pathway database (<http://www.genome.jp/kegg/pathway.html>).

Photosynthesis Analysis

For photosynthesis experiments, we used At-gCYP-3, At-gCYP-5, and wild-type plants growing in growth chambers operating at 16 h ~28°C d and 8 h ~25°C nights. We measured photosystem II maximum quantum efficiency (F_v/F_m) after transferring seedlings 4 d after germination to 15, 150, and 1100 $\mu\text{mol m}^{-2} \text{s}^{-1}$ of continuous white light for 10 d, detaching a single leaf from each of six seedlings per line, dark-adapting the detached leaves for 30 min, and imaging them with a CF imager (Technologica). We measured CO_2 uptake per unit leaf area also using plants at the onset of flowering using a LI-6400 portable photosynthesis system (LI-COR) fitted with a $2 \times 3\text{-cm}$ leaf chamber and a fixed LED light source using an array of red and blue LEDs. We determined light response curves for each sample at 380 ppm and 760 ppm CO_2 and nine light intensities from 0 to 2000 $\mu\text{mol m}^{-2} \text{s}^{-1}$ after an equilibration period of 1 h at a constant leaf temperature of 25°C, a chamber humidity of 50 to 55%, a CO_2 flow rate of 500 $\mu\text{mol s}^{-1}$, and an irradiance of 1500 $\mu\text{mol m}^{-2} \text{s}^{-1}$. We then logged CO_2 measurements from the middle of the flag leaves in triplicate, at steady state for each light intensity, with a minimum wait time of 120 s and maximum of 200 s.

Accession Numbers

Sequence data from this article can be found in the GenBank/EMBL data libraries under the accession numbers listed in Supplemental Table 10 online.

Supplemental Data

The following materials are available in the online version of this article.

Supplemental Figure 1. Two-Component Constructs.

Supplemental Figure 2. Heat Stress.

Supplemental Figure 3. Overexpression of a Chloroplast Protease.

Supplemental Table 1. All BR Metabolite Data.

Supplemental Table 2. P Values for BR Metabolite Data.

Supplemental Table 3. Epidermal Cell Sizes.

Supplemental Table 4. Leaves Killed by Heat Stress.

Supplemental Table 5. Statistical Analysis of Phenotype Data from Greenhouse-Grown Plants.

Supplemental Table 6. Statistical Analysis of Phenotype Data from Field-Grown Plants.

Supplemental Table 7. Statistical Analysis of Microarray Data.

Supplemental Table 8. Statistical Analysis of Microarray and qRT-PCR Data for Genes in Metabolic Pathways.

Supplemental Table 9. Statistical Analysis of Microarray and qRT-PCR Data for Photosynthesis Genes.

Supplemental Table 10. Accession Numbers.

Supplemental Data Set 1. Genes Differentially Expressed in Seedling Leaves.

Supplemental Data Set 2. Genes Differentially Expressed in Flag Leaves.

Supplemental Data Set 3. Genes Differentially Expressed in Seed.

ACKNOWLEDGMENTS

We thank Leonard Medrano for help with the GFP imaging, Andres Salazar for the microarrays, Charilyn Tejamo for the qRT-PCR, and Cailin Lei and Xin Zhang for help in the field. The research was partly funded by a Grant-in-Aid for Scientific Research (B) from the Ministry of Education, Culture, Sports, Science, and Technology of Japan (Grant 19380069) to S.F. and partly by Monsanto Corporation.

Received August 16, 2007; revised June 18, 2008; accepted July 25, 2008; published August 15, 2008.

REFERENCES

- Ashikari, M., Sakakibara, H., Lin, S., Yamamoto, T., Takashi, T., Nishimura, A., Angeles, E.R., Qian, Q., Kitano, H., and Matsuoka, M. (2005). Cytokinin oxidase regulates rice grain production. *Science* **309**: 741–745.
- Azpiroz, R., Wu, Y., LoCascio, J.C., and Feldmann, K.A. (1998). An Arabidopsis brassinosteroid-dependent mutant is blocked in cell elongation. *Plant Cell* **10**: 219–230.
- Bainbridge, K., Guyomarc'h, S., Bayer, E., Swarup, R., Bennett, M., Mandel, T., and Kuhlemeier, C. (2008). Auxin influx carriers stabilize phyllotactic patterning. *Genes Dev.* **22**: 810–823.
- Benjamini, Y., and Hochberg, Y. (1995). Controlling the false discovery rate: A practical and powerful approach to multiple testing. *J. R. Stat. Soc. B* **57**: 289–300.
- Boisnard-Lorig, C., Colon-Carmona, A., Bauch, M., Hodge, S., Doerner, P., Bancharrel, E., Dumas, C., Haseloff, J., and Berger, F. (2001). Dynamic analyses of the expression of the HISTONE:YFP fusion protein in Arabidopsis show that syncytial endosperm is divided in mitotic domains. *Plant Cell* **13**: 495–509.
- Bouvier-Navé, P., Husselstein, T., and Benveniste, P. (1998). Two families of sterol methyltransferases are involved in the first and the second methylation steps of plant sterol biosynthesis. *Eur. J. Biochem.* **256**: 88–96.
- Bürkle, L., Hibberd, J.M., Quick, P.W., Kühn, C., Hirner, B., and Frommer, W.B. (1998). The H⁺-sucrose cotransporter NtSUT1 is essential for sugar export from tobacco leaves. *Plant Physiol.* **118**: 59–68.
- Choe, S., Dilkes, B.P., Fujioka, S., Takatsuto, S., Sakurai, A., and Feldmann, K.A. (1998). The *DWF4* gene of Arabidopsis encodes a cytochrome P450 that mediates multiple 22 α -hydroxylation steps in brassinosteroid biosynthesis. *Plant Cell* **10**: 231–243.
- Choe, S., Fujioka, S., Noguchi, T., Takatsuto, S., Yoshida, S., and Feldmann, K.A. (2001). Overexpression of *DWARF4* in the brassinosteroid biosynthetic pathway results in increased vegetative growth and seed yield in Arabidopsis. *Plant J.* **26**: 573–582.
- Dhaubhadel, S., Browning, K.S., Gallie, D.R., and Krishna, P. (2002). Brassinosteroid functions to protect the translational machinery and heat-shock protein synthesis following thermal stress. *Plant J.* **29**: 681–691.
- Doust, A. (2007). Architectural evolution and its implications for domestication in grasses. *Ann. Bot. (Lond.)* **100**: 941–950.
- Fritzius, T., Aeschbacher, R., Wiemken, A., and Wingler, A. (2001). Induction of *ApL3* expression by trehalose complements the starch-deficient Arabidopsis mutant *adg2-1* lacking ApL1, the large subunit of ADP-glucose pyrophosphorylase. *Plant Physiol.* **126**: 883–889.
- Fujii, S., Hirai, K., and Saka, H. (1991). Growth-regulating action of brassinolide in rice plants. In *Brassinosteroids. Chemistry, Bioactivity, and Application*, H.G. Cutler, T. Yokota, and G. Adam, eds (Washington, DC: American Chemical Society), pp. 306–311.

- Fujioka, S., Choi, Y.-H., Takatsuto, S., Yokota, T., Li, J., Chory, J., and Sakurai, A.** (1996). Identification of castasterone, 6-deoxocastasterone, typhasterol and 6-deoxytyphasterol from the shoots of *Arabidopsis thaliana*. *Plant Cell Physiol.* **37**: 1201–1203.
- Fujioka, S., Takatsuto, S., and Yoshida, S.** (2002). An early C-22 oxidation branch in the brassinosteroid biosynthetic pathway. *Plant Physiol.* **130**: 930–939.
- Fujioka, S., and Yokota, T.** (2003). Biosynthesis and metabolism of brassinosteroids. *Annu. Rev. Plant Biol.* **54**: 137–164.
- Fujita, S., Ohnishi, T., Watanabe, B., Yokota, T., Takatsuto, S., Fujioka, S., Yoshida, S., Sakata, K., and Mizutani, M.** (2006). *Arabidopsis* CYP90B1 catalyses the early C-22 hydroxylation of C₂₇, C₂₈ and C₂₉ sterols. *Plant J.* **45**: 765–774.
- García-Lorenzo, M., Želisko, A., Jackowski, G., and Funk, C.** (2005). Degradation of the main photosystem II light-harvesting complex. *Photochem. Photobiol. Sci.* **4**: 1065–1071.
- Hiei, Y., Ohta, S., Komari, T., and Kumashiro, T.** (1994). Efficient transformation of rice (*Oryza sativa* L.) mediated by *Agrobacterium* and sequence analysis of the boundaries of the T-DNA. *Plant J.* **6**: 271–282.
- Hong, Z., Ueguchi-Tanaka, M., Fujioka, F., Takatsuto, S., Yoshida, S., Hasegawa, Y., Ashikari, M., Kitano, H., and Matsuoka, M.** (2005). The rice *brassinosteroid-deficient dwarf2* mutant, defective in the rice homolog of arabidopsis DIMINUTO/DWARF1, is rescued by the endogenously accumulated alternative bioactive brassinosteroid, dolichosterone. *Plant Cell* **17**: 2243–2254.
- Horton, P.** (2000). Prospects for crop improvement through the genetic manipulation of photosynthesis: Morphological and biochemical aspects of light capture. *J. Exp. Bot.* **51**: 475–485.
- Jiang, Y., and Wang, T.** (2006). Phytosterols in cereal by-products. *J. Am. Oil Chem. Soc.* **82**: 439–444.
- Johansson, H., Sterky, F., Amini, B., Lundberg, J., and Kleczkowski, L.A.** (2002). Molecular cloning and characterization of a cDNA encoding poplar UDP-glucose dehydrogenase, a key gene of hemicellulose/pectin formation. *Biochem. Biophys. Acta* **1576**: 53–58.
- Johnson, A.A.T., Hibberd, J.M., Gay, C., Essah, P.A., Haseloff, J., Tester, M., and Guiderdoni, E.** (2005). Spatial control of transgene expression in rice (*Oryza sativa* L.) using the GAL4 enhancer trapping system. *Plant J.* **41**: 779–789.
- Kleczkowski, L.A., Geisler, M., Ciereszko, I., and Johansson, H.** (2004). UDP-glucose pyrophosphorylase. An old protein with new tricks. *Plant Physiol.* **134**: 910–918.
- Knoester, M., van Loon, L.C., van den Heuvel, J., Hennig, J., Bol, J. F., and Linthorst, H.J.M.** (1998). Ethylene-insensitive tobacco lacks nonhost resistance against soil-borne fungi. *Proc. Natl. Acad. Sci. USA* **95**: 1933–1937.
- Kolbe, A., Tiessen, A., Schlupepmann, H., Paul, M., Ulrich, S., and Geigenberger, P.** (2005). Trehalose 6-phosphate regulates starch synthesis via posttranslational redox activation of ADP-glucose pyrophosphorylase. *Proc. Natl. Acad. Sci. USA* **102**: 11118–11123.
- Laplaze, L., Parizot, B., Baker, A., Ricaud, L., Martinière, A., Auguy, F., Franche, C., Nussaume, L., Bogusz, D., and Haseloff, J.** (2005). GAL4-GFP enhancer trap lines for genetic manipulation of lateral root development in *Arabidopsis thaliana*. *J. Exp. Bot.* **56**: 2433–2442.
- Li, X., et al.** (2003). Control of tillering in rice. *Nature* **422**: 618–621.
- Livak, K.J., and Schmittgen, T.D.** (2001). Analysis of relative gene expression data using real-time quantitative PCR and the $2^{-\Delta\Delta C_T}$ method. *Methods* **25**: 402–408.
- Misson, J., et al.** (2005). A genome-wide transcriptional analysis using *Arabidopsis thaliana* Affymetrix gene chips determined plant responses to phosphate deprivation. *Proc. Natl. Acad. Sci. USA* **102**: 11934–11939.
- Morinaka, Y., Sakamoto, T., Inukai, Y., Agetsuma, M., Kitano, H., Ashikari, M., and Matsuoka, M.** (2006). Morphological alteration caused by brassinosteroid insensitivity increases the biomass and grain production of rice. *Plant Physiol.* **141**: 924–931.
- Müssig, C., Fischer, S., and Altmann, T.** (2002). Brassinosteroid-regulated gene expression. *Plant Physiol.* **129**: 1241–1251.
- Nam, K.H., and Li, J.** (2002). BRI1/BAK1, a receptor kinase pair mediating brassinosteroid signaling. *Cell* **110**: 203–212.
- Nemhauser, J.L., Hong, F., and Chory, J.** (2006). Different plant hormones regulate similar processes through largely nonoverlapping transcriptional responses. *Cell* **126**: 467–475.
- Nemhauser, J.L., Mockler, T.C., and Chory, J.** (2004). Interdependency of brassinosteroid and auxin signaling in *Arabidopsis*. *PLoS Biol.* **2**: e258.
- Noguchi, T., Fujioka, S., Choe, S., Takatsuto, S., Yoshida, S., Yuan, H., Feldmann, K.A., and Tax, F.E.** (1999). Brassinosteroid-insensitive dwarf mutants of *Arabidopsis* accumulate brassinosteroids. *Plant Physiol.* **121**: 743–752.
- Peng, J., et al.** (1999). ‘Green revolution’ genes encode mutant gibberellin response modulators. *Nature* **400**: 256–261.
- Ramraj, V.M., Vyas, B.N., Godrej, N.B., Mistry, K.B., Swami, B.N., and Singh, N.** (1997). Effects of 28-homobrassinolide on yields of wheat, rice, groundnut, mustard, potato and cotton. *J. Agric. Sci.* **128**: 405–413.
- Reinhardt, B., Hänggi, E., Müller, S., Bauch, M., Wyrzykowska, J., Kerstetter, R., Poethig, S., and Fleming, A.J.** (2007). Restoration of *DWF4* expression to the leaf margin of a *dwf4* mutant is sufficient to restore leaf shape but not size: The role of the margin in leaf development. *Plant J.* **52**: 1094–2011.
- Ryoo, N., Yu, C., Park, C.S., Baik, M.Y., Park, I.M., Cho, M.H., Bho, S.H., An, G., Hahn, T.R., and Jeon, J.S.** (2007). Knockout of a starch synthase gene *OsSSIIIa/Flo5* causes white-core floury endosperm in rice (*Oryza sativa* L.). *Plant Cell Rep.* **26**: 1083–1095.
- Sakamoto, T., and Matsuoka, M.** (2004). Generating high-yielding varieties by genetic manipulation of plant architecture. *Curr. Opin. Biotechnol.* **15**: 144–147.
- Sakamoto, T., et al.** (2005). Erect leaves caused by brassinosteroid deficiency increase biomass production and grain yield in rice. *Nat. Biotechnol.* **24**: 105–109.
- Sasaki, A., Ashikari, M., Ueguchi-Tanaka, M., Itoh, H., Nishimura, A., Swapan, D., Ishiyama, K., Saito, T., Kobayashi, M., Khush, G.S., Kitano, H., and Matsuoka, M.** (2002). Green revolution: A mutant gibberellin-synthesis gene in rice. *Nature* **416**: 701–702.
- Satoh, H., Nishi, A., Yamashita, K., Takemoto, Y., Tanaka, Y., Hosaka, Y., Sakurai, A., Fujita, N., and Nakamura, Y.** (2003). Starch-branching enzyme I-deficient mutation specifically affects the structure and properties of starch in rice endosperm. *Plant Physiol.* **133**: 1111–1121.
- Schruff, M.C., Spielman, M., Tiwari, S., Adams, S., Fenby, N., and Scott, R.J.** (2006). The *AUXIN RESPONSE FACTOR 2* gene of *Arabidopsis* links auxin signalling, cell division, and the size of seed and other organs. *Development* **133**: 251–261.
- Scotfield, G.N., Hirose, T., Aoki, N., and Furbank, R.T.** (2007). Involvement of the sucrose transporter, OsSUT1, in the long-distance pathway for assimilate transport in rice. *J. Exp. Bot.* **58**: 3155–3169.
- Shimada, Y., Fujioka, S., Miyauchi, N., Kushiro, M., Takatsuto, S., Nomura, T., Yokota, T., Kamiya, Y., Bishop, G.J., and Yoshida, S.** (2001). Brassinosteroid-6-oxidases from *Arabidopsis* and tomato catalyze multiple C-6 oxidations in brassinosteroid biosynthesis. *Plant Physiol.* **126**: 770–779.
- Sjögren, L.L., Stanne, T.M., Zheng, B., Sutinen, S., and Clarke, A.K.** (2006). Structural and functional insights into the chloroplast ATP-dependent Clp protease in *Arabidopsis*. *Plant Cell* **18**: 2635–2649.
- Smart, C.M., Scotfield, S.R., Bevan, M.W., and Dyer, T.A.** (1991).

- Delayed leaf senescence in tobacco plants transformed with *tmr*, a gene for cytokinin production in *Agrobacterium*. *Plant Cell* **3**: 647–656.
- Smidansky, E.D., Clancy, M., Meyer, F.D., Lanning, S.P., Blake, N.K., Talbert, L.E., and Giroux, M.J.** (2002). Enhanced ADP-glucose pyrophosphorylase activity in wheat endosperm increases seed yield. *Proc. Natl. Acad. Sci. USA* **99**: 1724–1729.
- Smith, J.R., and Nelson, R.L.** (1986). Relationship between seed-filling period and yield among soybean breeding lines. *Crop Sci.* **26**: 469–472.
- Smyth, G.K., Michaud, J., and Scott, H.S.** (2005). Use of within-array replicate spots for assessing differential expression in microarray experiments. *Bioinformatics* **21**: 2067–2075.
- Symons, G.M., and Reid, J.B.** (2004). Brassinosteroids do not undergo long-distance transport in pea. Implications for the regulation of endogenous brassinosteroid levels. *Plant Physiol.* **135**: 2196–2206.
- Szekeres, M., Németh, K., Koncz-Kálmán, Z., Mathur, J., Kauschmann, A., Altmann, T., Rédei, G.P., Nagy, F., Schell, J., and Koncz, C.** (1996). Brassinosteroids rescue the deficiency of CYP90, a cytochrome P450, controlling cell elongation and de-etiolation in *Arabidopsis*. *Cell* **85**: 171–182.
- Takeda, T., Suwa, Y., Suzuki, M., Kitano, H., Ueguchi-Tanaka, M., Ashikari, M., Matsuoka, M., and Ueguchi, C.** (2003). The *OsTB1* gene negatively regulates lateral branching in rice. *Plant J.* **33**: 513–520.
- Tanabe, S., Ashikari, M., Fujioka, S., Takatsuto, S., Yoshida, S., Yano, M., Yoshimura, A., Kitano, H., Matsuoka, M., Fujisawa, Y., Kato, H., and Iwasaki, Y.** (2005). A novel cytochrome P450 is implicated in brassinosteroid biosynthesis via the characterization of a rice dwarf mutant, *dwarf11*, with reduced seed length. *Plant Cell* **17**: 776–790.
- Wang, J., Jiang, J., and Oard, J.H.** (2000). Structure, expression and promoter activity of two polyubiquitin genes from rice (*Oryza sativa* L.). *Plant Sci.* **156**: 201–211.
- Wang, R., Okamoto, M., Xing, X., and Crawford, N.M.** (2003). Microarray analysis of the nitrate response in *Arabidopsis* roots and shoots reveals over 1,000 rapidly responding genes and new linkages to glucose, trehalose-6-phosphate, iron, and sulfate metabolism. *Plant Physiol.* **132**: 556–567.
- Wingler, A., Fritzius, T., Wiemken, A., Boller, T., and Aeschbacher, R.A.** (2000). Trehalose induces the ADP-glucose pyrophosphorylase gene, *ApL3*, and starch synthesis in *Arabidopsis*. *Plant Physiol.* **124**: 105–114.
- Wood, C.C., Robertson, M., Tanner, G., Peacock, W.J., Dennis, E.S., and Helliwell, C.A.** (2006). The *Arabidopsis thaliana* vernalization response requires a polycomb-like protein complex that also includes VERNALIZATION INSENSITIVE 3. *Proc. Natl. Acad. Sci. USA* **103**: 14631–14636.
- Wu, C., Adach, T., Hatano, T., Washida, H., Suzuki, A., and Takaiwa, F.** (1998). Promoters of rice seed storage protein genes direct endosperm-specific gene expression in transgenic rice. *Plant Cell Physiol.* **39**: 885–889.
- Xu, D., Lei, M., and Wu, R.** (1995). Expression of the rice *Osgrp1* promoter-Gus reporter gene is specifically associated with cell elongation/expansion and differentiation. *Plant Mol. Biol.* **28**: 455–471.
- Xu, H.L.** (2007). Effects of exogenous epibrassinolide and abscisic acid on grain yield of sorghum plants growing under soil water deficit. In *Dryland Crop Production: Technology Breakthroughs and Study Cases*, H.L. Xu, ed (Trivandrum, India: Research Signpost), pp. 195–202.
- Yokota, T., Higuchi, K., Kosaka, Y., and Takahashi, N.** (1992). Transport and metabolism of brassinosteroids in rice. In *Progress in Plant Growth Regulation*, C.M. Karssen, L.C.V. Loon, and D. Vreugdenhil, eds (Dordrecht, The Netherlands: Kluwer), pp. 298–305.
- Yu, J.Q., Huang, L.F., Hu, W.H., Zhou, Y.H., Mao, W.H., Ye, S.F., and Nogués, S.** (2004). A role for brassinosteroids in the regulation of photosynthesis in *Cucumis sativus*. *J. Exp. Bot.* **55**: 1135–1143.
- Zhang, L., and Guarente, L.** (1994). The yeast activator HAP1 – a GAL4 family member – binds DNA in a directly repeated orientation. *Genes Dev.* **8**: 2110–2119.
- Zou, J., Chen, Z., Zhang, S., Zhang, W., Jiang, G., Zhao, X., Zhai, W., Pan, X., and Zhu, L.** (2005). Characterizations and fine mapping of a mutant gene for high tillering and dwarf in rice (*Oryza sativa* L.). *Planta* **222**: 604–612.
- Zou, J., Zhang, S., Zhang, W., Li, G., Chen, Z., Zhai, W., Zhao, X., Pan, X., Xie, Q., and Zhu, L.** (2006). The rice *HIGH-TILLERING DWARF1* encoding an ortholog of *Arabidopsis* MAX3 is required for negative regulation of the outgrowth of axillary buds. *Plant J.* **48**: 687–698.

Brassinosteroids Regulate Grain Filling in Rice

Chuan-yin Wu, Anthony Trieu, Parthiban Radhakrishnan, Shing F. Kwok, Sam Harris, Ke Zhang, Jiulin Wang, Jianmin Wan, Huqu Zhai, Suguru Takatsuto, Shogo Matsumoto, Shozo Fujioka, Kenneth A. Feldmann and Roger I. Pennell

PLANT CELL 2008;20;2130-2145; originally published online Aug 15, 2008;

DOI: 10.1105/tpc.107.055087

This information is current as of October 16, 2008

Supplemental Data	http://www.plantcell.org/cgi/content/full/tpc.107.055087/DC1
References	This article cites 66 articles, 37 of which you can access for free at: http://www.plantcell.org/cgi/content/full/20/8/2130#BIBL
Permissions	https://www.copyright.com/ccc/openurl.do?sid=pd_hw1532298X&iissn=1532298X&WT.mc_id=pd_hw1532298X
eTOCs	Sign up for eTOCs for <i>THE PLANT CELL</i> at: http://www.plantcell.org/subscriptions/etoc.shtml
CiteTrack Alerts	Sign up for CiteTrack Alerts for <i>Plant Cell</i> at: http://www.plantcell.org/cgi/alerts/ctmain
Subscription Information	Subscription information for <i>The Plant Cell</i> and <i>Plant Physiology</i> is available at: http://www.aspb.org/publications/subscriptions.cfm